https://doi.org/10.5194/egusphere-2026-4082
Preprint. Discussion started: 21 July 2026

Medical deserts induced by pluvial flood: emergency medical accessibility loss and population exposure

Yating Yang[1,2], Xiaodong Guo[1], Lu Han[2], Chenhong Xia[1], Zhitao Wang[1]

[1]College of Architecture and Urban Planning, Beijing University of Technology, Beijing 100124, China
[2]College of Urban Construction, Hebei Normal University of Science & Technology, Qinhuangdao 066000, China

Correspondence to: Xiaodong Guo (guoxd7797@163.com)

Abstract. Pluvial floods increasingly threaten emergency medical systems (EMS) by disrupting road networks. Previous studies have examined flood impacts on roads and EMS separately, neglecting population distribution. This study evaluates EMS accessibility loss and flood-induced medical deserts under pluvial floods in Mentougou New Town. Flood inundation under 10-, 20-, 50-, and 100-year return periods is simulated using MIKE FLOOD. The the simulated water depths are used to adjust travel speeds and identify interrupted road segments. Based on the resulting travel-time matrices, 8-min service areas are calculated and overlaid with high-resolution population data. The results reveal that flood risk exhibits nonlinear growth characteristics, with the 50-year return period rainfall event representing a critical threshold. Under the 50-year event, several key roads begin to fail, and the EMS coverage area contracts sharply. Under the 100-year event, large flood-induced medical deserts appear in old urban districts, high-density residential communities, and peripheral industrial zones. These areas form where road disruption, concentrated population, and limited alternative access overlap. The findings demonstrate that road-network failure and population exposure must be assessed jointly when evaluating flood impacts on EMS, supporting emergency planning, critical road protection, and resilient medical resource allocation in flood-prone cities.

1 Introduction

Extreme precipitation events have become more frequent and intense under global warming, posing a serious and growing challenge to urban disaster risk management (Abebe et al., 2025; Madakumbura et al., 2021). Pluvial flood is often triggered by short-duration, high-intensity rainfall that exceeds the drainage capacity of urban systems (Haghighatafshar et al., 2020). It can rapidly generate surface runoff, localized waterlogging, and road inundation in built-up areas. Such processes do not only produce direct physical damage but also disrupt critical infrastructure systems, including transport, emergency response, and healthcare services (Chang et al., 2010; Karamouz et al., 2019; Xie et al., 2024). For urban disaster risk reduction, it is necessary to examine not only the spatial extent of inundation but also the cascading consequences of flooding for essential public services (Emami et al., 2024).

Emergency medical services (EMS) are among the most time-sensitive urban functions affected by pluvial flood (Yang et al., 2020). Since pre-hospital care relies on rapid ambulance response and patient transport, a central task of EMS is to reduce the time needed to reach appropriate medical facilities (Green et al., 2017). During flood events, hospitals may remain operational but become difficult to access when road inundation reduces travel speeds, blocks key links, or increases detour costs (Gou et al., 2022; He et al., 2026b). Previous studies have provided useful methods for assessing flood-induced transport disruption, including hydrodynamic simulation, road failure thresholds, speed reduction functions, and network indicators (Al-Qadami et al., 2024; Chen and Yang, 2011; Hudson et al., 2019; Patro et al., 2009). However, these road-level impacts need to be further translated into changes in service areas and accessibility for EMS,.

The effects of pluvial flood are shaped not only by inundation depth, but also by the populations, and services exposed to the hazard. Following the Intergovernmental Panel on Climate Change risk concept, pluvial flood risk can be understood as the combined effect of hazard, exposure, and vulnerability (IPCC, 2014; Vogelbacher et al., 2026). Hazard refers to the intensity and spatial extent of flooding, exposure refers to people and infrastructure located in affected areas, and vulnerability describes the degree to which exposed people or systems may suffer damage (Rufat et al., 2015; Tate et al., 2021). Recent studies have therefore emphasized the need to consider flood exposure, social vulnerability, and access to essential services together (Ermagun et al., 2024). This perspective is particularly relevant for EMS, because flood risk is not limited to physical inundation; it also depends on whether residents can still reach care, medication, and emergency treatment.

In this study, population distribution represents exposure and potential emergency demand (Tate et al., 2021). High-density residential areas indicate where many people may be affected if emergency access is interrupted. The vulnerability of EMS access depends on the relationship between population, roads, and hospitals (Gangwal et al., 2023a; Liu et al., 2023). Disaster-induced infrastructure disruptions can increase travel times to healthcare facilities and change the service options available to residents. This issue is especially important for EMS, as adverse weather and flood events can reduce accessibility and response coverage (Zhang et al., 2024). When communities rely on a limited number of roads or lack nearby alternative facilities, pluvial flood can turn a transport disruption into a healthcare access problem. The concept of medical deserts provides a way to describe this problem. Medical deserts usually refer to areas with insufficient access to healthcare resources under normal conditions (Behrman et al., 2021; Brînzac et al., 2024). During pluvial flood, however, medical deserts may also appear temporarily when road-network disruption prevents high-density populations from reaching hospitals within critical response times (Papilloud et al., 2024). These flood-induced medical deserts are not simply areas far away from hospitals. They form where flood hazard, population exposure, road-network vulnerability, and limited medical alternatives overlap.

Existing studies have developed methods for simulating pluvial flood hazards, assessing road-network disruption, and evaluating EMS accessibility. However, flood impact studies have mainly addressed inundation extent and road-network performance, whereas EMS accessibility studies commonly evaluate service coverage without explicitly incorporating scenario-dependent changes in road passability and travel speed. This makes it difficult to identify the rainfall intensity at which flood-induced road degradation leads to substantial EMS accessibility loss, or to determine which high-density communities are most likely to lose timely access to hospitals. This limitation is particularly important for analysing flood-induced medical deserts, which arise from the spatial overlap of inundation, road-network vulnerability, hospital distribution, and population exposure. An integrated assessment is therefore needed to link pluvial flood intensity, dynamic travel conditions, EMS coverage areas, and exposed populations within a consistent analytical framework.

Motivated by these observations, this study develops an integrated assessment framework to evaluate EMS accessibility and analyse the spatial emergence of medical deserts under pluvial flooding. The framework links flood inundation, road-network degradation, EMS accessibility, and population exposure to assess EMS accessibility loss, service-area contraction, and population exposure to emergency care deficits under the increasing flood intensity. Based on the EMS coverage areas, population data are overlaid with hospital accessibility results to identify flood-induced medical deserts where high-density communities lose timely access to emergency medical care. The main contribution of this study is to translate pluvial flood impacts from physical inundation and road disruption into population-level EMS accessibility deficits. The study identifies temporary medical deserts in high-density areas where inundation-related road disruption and limited medical alternatives lead to the loss of timely hospital access. It also documents a nonlinear decline in EMS accessibility as rainfall severity increases, with marked contraction of effective hospital service areas under severe flood events. The findings inform emergency preparedness, critical road segment protection, and resilient medical resource allocation in flood-prone urban areas.

2 Study area and data resources

2.1 Study area

https://doi.org/10.5194/egusphere-2026-4082
Preprint. Discussion started: 21 July 2026

The eastern new urban district of Mentougou, Beijing, hereafter referred to as Mentougou New Town, is selected as the study area (Fig. 1). The area represents a typical piedmont urban setting where plain built-up districts, valley-transition zones, old urban neighbourhoods, and newly developed residential areas coexist. This spatial structure is common in the urban fringe of many mountainous and hilly cities. In such areas, older districts often have dense and narrow street networks, while newer residential zones are connected to the urban core by a limited number of main corridors. These conditions make the case useful for examining emergency service accessibility in cities with uneven road connectivity and concentrated public service facilities. The road network in the study area consists of 656 road segments. The area has eight hospitals, including secondary and tertiary facilities, which serve as the main supply nodes for emergency medical response. The combination of centralized medical resources, heterogeneous road conditions, and uneven population distribution makes Mentougou New Town a representative case for studying flood-induced EMS accessibility loss in piedmont urban areas.

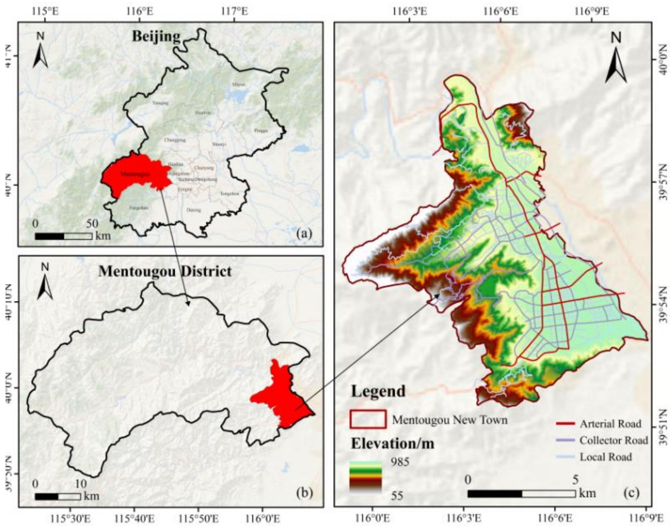

Figure 1: General situation of the study area. (a) Location of Mentougou District in Beijing. (b) Location of Mentougou New Town in Mentougou District. (c) Topography of Mentougou New Town.

2.2 Data resources

To support the integrated spatiotemporal modeling, Table 1 summarizes the multi-source datasets utilized in this study. Specifically, hydrometeorological, topographic, and sewer system data are used to simulate the flood inundation extent; road network data serve to construct the transportation network topology and evaluate traffic capacity. Hospital data represent the post-disaster supply capacity; and high-resolution population distribution data characterize the dynamic healthcare demand.

Table 1: List of basic data required for the study.

Data Category	Description	Source
Hydrometeorological data	Historical daily rainfall	China Meteorological Data Network (https://data.cma.cn/)
Topographic data	Elevation	Geospatial Data Cloud (https://www.gscloud.cn/)
River data	Water system distribution	National Geomatics Center of China (https://www.geodata.cn/)
Sewer system data	Design return period, elevations, etc.	Government water resources authority, field survey
Road network data	Road name, length, classification, etc	Government transport authority, field survey
Hospital data	Location, facility level	POI (Point of Interest) coordinates, field survey
Population data	Population density distribution	WorldPop (https://hub.worldpop.org/)

https://doi.org/10.5194/egusphere-2026-4082
Preprint. Discussion started: 21 July 2026

3 Methods

This section introduces the methodology for evaluating EMS capability and spatial mismatch. This study proceeds along four analytical dimensions: pluvial flood simulation, road network assessment, EMS coverage quantification, and spatial supply-demand matching. As illustrated in Fig. 2, the research framework follows a four-step procedure. (1) Inundation areas of pluvial flood with different return period rainfall events (10-year, 20-year, 50-year, and 100-year) are simulated with the MIKE FLOOD model. (2) A topological road network is first constructed; then, by overlaying the inundation results and applying a depth-dependent speed reduction function to travel speeds, the traffic capacity levels and travel time matrix of roads are quantified. (3) Based on the traffic capacity and travel time matrix, a GIS-based service area analysis is conducted to quantify the area which patients can reach hospitals in the 8-minute spatial extent within. (4) This dynamic service coverage is then overlaid with high-density population distribution data to reveal the spatial mismatch patterns of medical deserts. Detailed descriptions of these steps are provided in Sections 3.1-3.3.

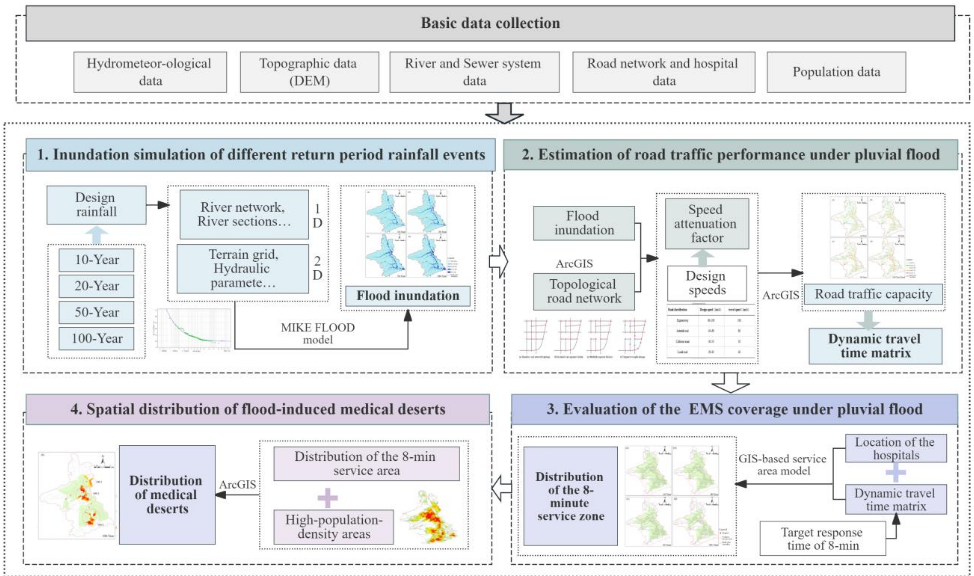

Figure 2: Research framework of this study.

3.1 Inundation simulation under different return period rainfall events

Multi-scenario flood simulation is the foundation of this study. The MIKE FLOOD model is selected for its advantage in overcoming the limitations of single models in computational accuracy and spatial resolution (Pareta and Pareta, 2025; Patro et al., 2009) . A one-dimensional (1D) model is established for the drainage network and river system, with sub-catchments delineated and composite runoff coefficients determined per the Beijing Design Standard (Table 2). The composite runoff coefficient of each sub-catchment was then calculated using an area-weighted method. A two-dimensional (2D) surface model is built on a 2-m DEM (1:5000), with building and road footprints incorporated to delineate impervious boundaries. Design rainfall for four return periods (10-year, 20-year, 50-year, and 100-year) is derived from the Pearson type III distribution, and hyetographs are constructed following the Zone II rainstorm pattern in the Beijing Hydrological Handbook. The 1D and 2D models are dynamically coupled via overflow outlets and river cross-sections at a 30-s time step to enable bidirectional water exchange. Model accuracy is verified against field-measured inundation depths at three sites from the July 2023 extreme rainfall event in Mentougou New Town. Model accuracy is verified against field-measured inundation depths at three sites from the July, 2023 extreme rainfall event in Mentougou New Town. After iterative parameter refinement, relative errors are within 10%.

https://doi.org/10.5194/egusphere-2026-4082
Preprint. Discussion started: 21 July 2026

Table 2: Comprehensive runoff coefficients of typical urban areas.

Typical urban area	Composite runoff coefficient
Concentrated residential zones	0.65
Suburban residential areas	0.35
Legacy low-rise housing	0.89
Public facility clusters	0.75
Industrial zones	0.65
Green spaces	0.35

(Source of table: Beijing *Urban Stormwater System Planning and Design Storm Runoff Calculation Standard*)

3.2 Estimation of road traffic performance under pluvial flood

Based on the simulation results in Section 3.1, a topological network of the roads is first constructed using ArcGIS (Golazad et al., 2024). The impacts of flood inundation on road networks are further analyzed, including failures of isolated road segments, the simultaneous failure of multiple segments, and the changes in segment weights caused by different inundation depths (Fig. 3).

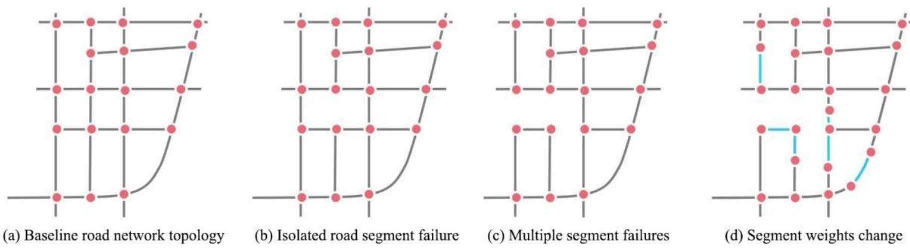

Figure 3: Road sections and topology structure changes at (a) baseline road network topology; (b) isolated road segment failure; (c) multiple segment failures; and (d) segment weights changes.

Subsequently, the relationship between inundation depth and road traffic capacity must be further defined (Fang and Gu, 2026). Regnolato et al (2017) employed curve-fitting methods to reveal the relationship between road inundation depth and vehicle travel speed. Chen et al. (2024) further analyzed the correlation between maximum safe driving speeds and water depths specifically for large vehicles such as ambulances. Thus, this study assumes that traffic is interrupted when the inundation depth exceeds 0.5 m. For road segments with water depth below 0.5 m, a speed reduction model is used to determine the coefficient of speed reduction (Zhu et al., 2025). Consequently, the traffic performance of road network is classified into five levels (I, II, III, IV, V), where Level I represents the best and Level V the worst (Table 3).

Table 3: Road traffic performance under different inundation depths.

Inundation depth (m)	**Inundation status**	**Speed attenuation factor**	**Impairment status**	**Road traffic performance**
<0.05	Shallow	0.9-1.0	Negligible	Level I
0.05-0.15		0.6-0.9	Slight	Level II
0.15-0.3	Medium	0.3-0.6	Moderate	Level III
0.3-0.5		0.1-0.3	Extensive	Level IV
＞0.5	Deep	0-0.1	Complete	Level V

The actual road performance during disasters is calculated using Eq. (1), and the travel time cost per segment is converted via Eq. (2).

$$C_i^t = C_i^0 \times \alpha\left(h_i^t\right) \tag{1}$$

$$T_i^t = \frac{L_i}{v_i^0 \times \alpha\left(h_i^t\right)} \tag{2}$$

https://doi.org/10.5194/egusphere-2026-4082
Preprint. Discussion started: 21 July 2026

Where C_i^t is the actual travel speed of road segment i at time t, C_i^0 is the design speed of the road segment (km/h), $\alpha\left(h_i^t\right)$ denotes the speed reduction coefficient corresponding to the inundation depth of road segment i at time t. T_i^t is the travel time of the road segment i at time t (min); L_i is the length of road segment i (km); v_i^0 refers to the design speed of road segment (km/h). The parameter C_i^0 denotes the design speeds in the Code for Design of Urban Road Engineering (CJJ 37-2012), with detailed values listed in Table 4. Finally, ArcGIS is applied to overlay the inundation raster data with the road network, and a dynamic travel time matrix is generated for various return period rainfall events, which serves as the core input variable for the accessibility analysis of EMS.

Table 4: Design speeds and operating speeds by road class.

Road classification	Design speed (km/h)	Travel speed (km/h)
Expressway	60-100	100
Arterial road	40-60	60
Collector road	30-50	50
Local road	20-40	40

3.3 Evaluation of 8-min EMS coverage under pluvial flood

Building upon the dynamic travel time matrix established in Section 3.2, the subsequent step is to evaluate the EMS coverage. EMS response is generally considered optimal when arrival occurs within 8-10 minutes (Green et al., 2017). Yin (2018) showed that the coverage of EMS within the 8-min threshold exhibits significant spatial heterogeneity under pluvial flood. Thus, this study sets 8-min as the target for emergency medical response. This study therefore use 8-min as the target emergency medical response threshold. By integrating this threshold with the dynamic travel-time matrix and inundation data, a GIS-based service area model is used to delineate hospital service boundaries.

The procedure involved two steps. First, a dynamic network dataset is constructed. Based on the road network topology, the travel times in pluvial flood are added as attribute fields via spatial joining to couple the network with its disaster-affected states. Second, a service area analysis layer is created. A new service area layer is generated, medical facility locations are loaded, and an 8-minute rescue time threshold is established. Starting from hospitals, travel times are accumulated along the least-cost paths until the predefined threshold is reached, thereby delineating the service area boundaries. Compared with conventional fixed-radius static models, this method incorporates road topology and traffic conditions to reflect dynamic changes in EMS coverage.

3.4 Spatial distribution of medical deserts

Based on the method detailed in Sections 3.1 to 3.3, the dynamic physical boundaries of EMS coverage with different return period rainfall events are delineated. Actually, the crucial determinant of rescue efficiency lies in the spatial interaction between population distribution and EMS coverage. To identify high-density areas with insufficient medical services, known as medical deserts (Brînzac et al., 2024), this study employs high-resolution population distribution data from the 2025 China population dataset provided by WorldPop, which features a spatial resolution of 100 m.

First, the vector service area layers for each event are converted into binary rasters with the same resolution as the population data (assigned 1 within the service area and 0 outside). The population distribution outside the service area is then extracted using a raster calculator. In this study, high-population-density areas are defined as grid cells with a density exceeding the average population density of the study area. Finally, grid cells with densities above this average are filtered through a raster calculation to generate a binary raster of high-population-density zones (Eq. 3).

$$P_{out} = P_{grid} \times \left(1 - S_{grid}\right) \tag{3}$$

https://doi.org/10.5194/egusphere-2026-4082
Preprint. Discussion started: 21 July 2026

Where: P_{out} denotes the population distribution outside the service area; P_{grid} represents the population raster (representing the number of people in each grid cell); S_{grid} is the binary service area raster, where cells within the service area are assigned a value of 1, and those outside are assigned 0.

Second, by overlaying the conditions of "outside the service area" and "high-population-density zones" , grid cells that simultaneously satisfy both criteria are defined as medical deserts.

$$M_{desert} = \left(S_{raster} = 0\right) \cap \left(D_{raster} \geq D_{avg}\right) \tag{4}$$

Where the M_{desert} is the medical desert raster, representing areas with high population density but no medical service coverage; S_{raster} denotes the service area raster, where a value of 0 indicates areas outside the emergency medical service range; D_{raster} represents the population density raster; D_{avg} refers to the average population density of the study area.

4 Results

4.1 Results of inundation simulation under different return period rainfall events

Based on the simulation results and statistical analysis, this study quantifies the inundation evolution patterns under four typical rainfall return periods. The spatial distribution is shown in Fig. 4, and the statistical data are presented in Table 5.

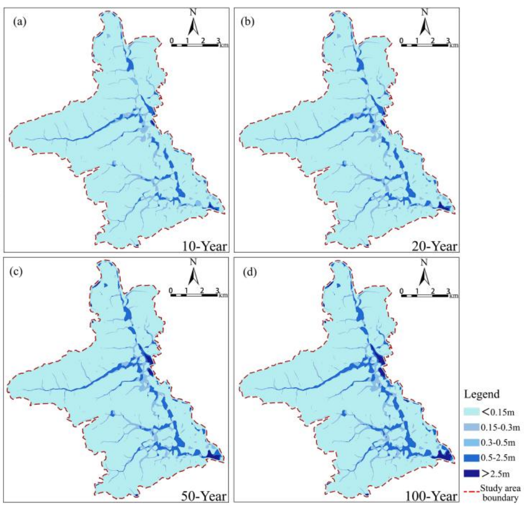

Figure 4: Inundation depths under (a) the 10-year; (b) 20-year; (c) 50-year; and (d) 100-year return period rainfall events.

The results demonstrate that inundation extent exhibits significant non-linear characteristics. The growth rate of total inundated area is 10.05% between 10-year and 20-year, jumps sharply to 32.74% between 20-year and 50-year, and moderates to 15.73% between 50-year and 100-year, yet remains high. This suggests that beyond the 50-year return period, inundation extent becomes increasingly sensitive to hazard intensification, leading to non-linear accumulation of systemic risk.

Table 5: Statistics of inundated areas by depth category.

Return period	0.05-0.15m		0.15-0.3m		0.3-0.5m		>0.5m	
	Area (km²)	Proportion (%)	Area (km²)	Proportion (%)	Area (km²)	Proportion (%)	Area (km²)	Proportion (%)
10-year	13.54	15.56	3.74	4.30	2.67	3.07	3.24	3.72
20-year	14.72	16.92	4.28	4.92	2.48	2.85	4.04	4.64
50-year	17.77	20.43	5.29	6.08	3.53	4.06	7.03	8.08
100-year	19.6	22.53	5.15	6.84	4.26	4.90	9.9	11.38

https://doi.org/10.5194/egusphere-2026-4082
Preprint. Discussion started: 21 July 2026

As shown in Table 5, shallow inundation (0.05-0.15 m) maintains the largest share, its proportion increases only moderately from 15.56% to 22.53%, indicating weakening dominance. In contrast, the proportion of deep inundation (>0.5 m) rises sharply from 3.72% (10-year) to 11.38% (100-year), more than a three-fold increase, with the corresponding area expanding from 3.24 km² to 9.9 km², representing the largest increase among all depth categories. In summary, intensifying pluvial flood is manifested not only in a larger total inundated area, but also in a marked increase in deep-inundated zones. This substantially affects EMS accessibility and directly shapes the spatial severity of subsequent road disruptions.

4.2 Road network disruption

The road network of Mentougou New Town contains 656 road segments, with a total length of 289.38 km. The inundation results in Section 4.1 were spatially overlaid with the road network to calculate the length of roads exposed to different inundation depths. Table 6 summarises road inundation data across return period events. The proportion of deeply inundated roads increases from 3.90% in the 10-year event to 10.27% in the 100-year event, indicating a substantial increase in road segments likely to experience severe passability loss.

Table 6: Statistics of road segments by inundation severity.

Return period	Shallow inundation		Moderate inundation		Deep inundation	
	Cumulative length (km)	Proportion (%)	Cumulative length (km)	Proportion (%)	Cumulative length (km)	Proportion (%)
10-year	42.49	14.68	28.83	9.96	11.28	3.90
20-year	44.73	15.46	30.44	10.52	13.11	4.53
50-year	49.58	17.13	37.20	12.86	23.01	7.95
100-year	45.49	15.72	36.40	12.58	29.71	10.27

Based on these results, the spatial composition of roads with varying traffic capacity is examined (Fig. 5 and 6). Under the 10-year and 20-year events, road network performance remains relatively stable, with only minor efficiency reductions and intact overall connectivity. With a 50-year return period rainfall event, structural risks emerge. The proportion of Level I roads drops from 54.78% to 48.61%, while Level IV and V roads increase from 11.62% to 19.24%, indicating accelerated connectivity decay and substantially reduced rescue route redundancy. As for the 100-year return period, Level I roads further shrink to 45.82%, and low-efficiency or failed roads continue to increase, dominating the network and markedly decreasing overall connectivity efficiency and reliability.

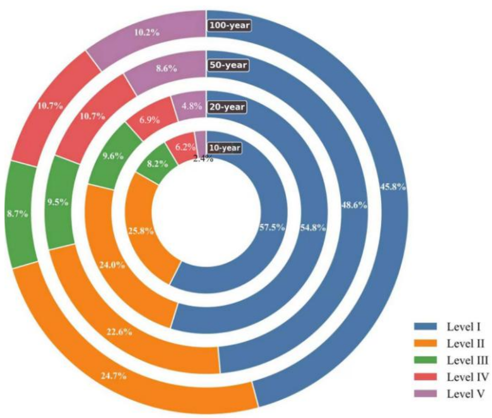

Figure 5: Proportions of roads by traffic performance level.

Further analysis reveals that the southern region, already characterized by insufficient medical facilities, relies heavily on a limited number of crucial roads for service access. When these crucial roads are among the first to be inundated, EMS of this area are significantly affected.

https://doi.org/10.5194/egusphere-2026-4082
Preprint. Discussion started: 21 July 2026

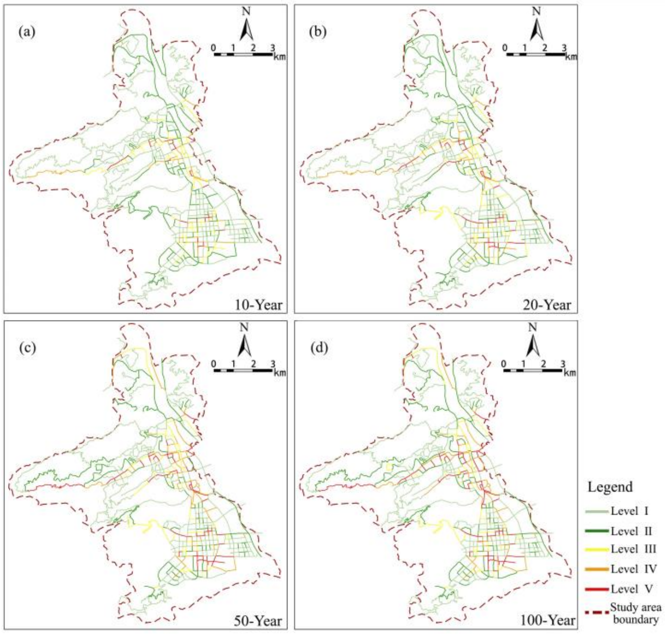

Figure 6: Road traffic performance levels under (a) the 10-year; (b) 20-year; (c) 50-year; (d) 100-year return period rainfall events.

4.3 Decay patterns and vulnerability identification of EMS

Changes in road network performance lead to corresponding changes in 8-min EMS coverage areas (Fig. 7). Regarding spatial distribution, the coverage of EMS withen 8 min exhibits a three-stage attenuation pattern: characterized sequentially by peripheral decay, core fragmentation, and eventual discrete degradation. These areas are minimally affected under common pluvial flood. However, the EMS coverage undergoes significant contraction when the 50-year and 100-year return period rainfall events occur.

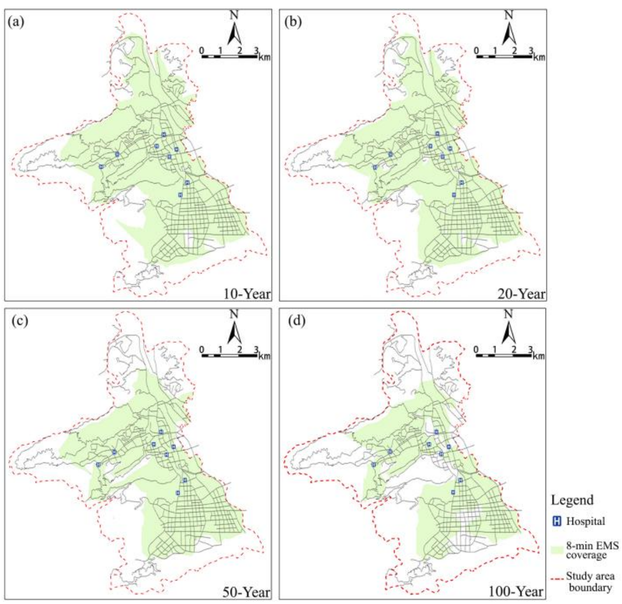

Figure 7: Distribution of 8-min EMS coverage under (a) the 10-year; (b) 20-year; (c) 50-year; and (d) 100-year return period rainfall events.

https://doi.org/10.5194/egusphere-2026-4082
Preprint. Discussion started: 21 July 2026

As summarized in Table 7, under the 10-year event, EMS can cover almost all built-up areas in the study area within 8 min. Under the 20-year event, the extent of vulnerable zones expands slightly, with the service area reduction remaining below 2%. Under the 50-year event,, the originally continuous and integrated core service areas begin to undergo fragmentation.. The 8-min EMS coverage area shrink to 42.31 km², representing an 18.7% reduction compared with the 10-year. Vulnerable zones expand from the periphery toward the near-core regions, with certain areas degrading inaccessible within 8 minutes. The primary reason is the localized failure of road segments where water depths exceed operational thresholds, causing a surge in the time cost for detouring. This highlights the inadequate flood resilience of critical road segments surrounding the core area.

Table 7: Statistics of the 8-min EMS coverage areas under different events.

Return period	the coverage of EMS within 8-min (km²)	Proportion (%)
10-year	52.06	59.84
20-year	51.25	58.91
50-year	42.31	48.63
100-year	32.36	37.2

In the 100-year return period, the 8-minute service zone further contracts by 23.5% relative to the 50-year, accounting for only 37.2% of the total study area. This research finds that the transition of service zone from a continuous to a discrete state is not random. It is actuated by the failure of a small number of roads with high betweenness centrality (e.g. Binhe Road, Dayu South Road, and Mentougou Road). Although these roads represent only 3.2% of the total network length, their failure causes a 61% decline in global network efficiency. This indicates that the damage to a few key roads causes a cascading failure of EMS. Although these roads represent only 3.2% of the total network length, their failure causes a 61% decline in global network efficiency. This indicates that the damage to a few key roads causes a cascading failure of EMS.

4.4 Spatial distribution of medical deserts

This study identifies the spatial mismatch between high-population-density zones and 8-min EMS coverage areas. Under the 10-year and 20-year events, high-density populations are largely covered by EMS, with fewer than 5% of high-density grid cells outside the service area are sparsely distributed along the periphery. As showen in Fig. 8a, when the rainfall return period increases to 50-year, a shift occurs in the service deprivation of high-density populations. The unserved population reaches 70,000, accounting for 21.46% of the total population of the New Town (326,000). The contraction of EMS coverage results in three flood-induced temporary medical deserts, labeled 50-1, 50-2 and 50-3, with areas of 146.99 ha,18.92 ha and 58.94 ha. Under the 100-year event (Fig. 8b), service gaps for high-density populations widen further . The unserved high-density populations rise to 195,500, representing 59.97% of the total populations. Three large contiguous medical deserts are formed (100-1, 100-2, and 100-3), with areasof 112.79 ha, 216.74 ha, and 259.26 ha, collectively covering 31.7% of the high-density zones. These regions correspond to the main service gaps left by the contracted EMS coverage, and their boundaries are consistent with the road interruption points shown in Fig. 6d.

Medical facilities in Mentougou New Town are concentrated mainly in the central area. This concentration creates a dual disadvantage for the 100-1 and 100-2 clusters, which are located away from the medical core: they experience both reduced accessibility caused by road-network failure and limited alternative service options due to the distance from medical facilities. The spatial association between land use and medical deserts is further analyzed. Medical desert 100-1 is located in an old urban district close to the core hospital. However, the road hierarchy in the old district is low and the disruption of Mentougou Road, and the waterlogging on branch roads restrict traffic speeds. Medical desert 100-2 is a core residential zone with a high population density and the damage of two main arterials leading to major hospitals creates a gap in the originally continuous service area. Medical desert 100-3 is mainly located in an industrial park which is far from hospitals.

https://doi.org/10.5194/egusphere-2026-4082
Preprint. Discussion started: 21 July 2026

The disruption of Shidan Road further aggravates the systemic risks of EMS. The spatial correspondence between medical deserts and inundated roads in Fig. 6 demonstrates that road interruption is a key mechanism through which pluvial flooding reduces emergency medical access. Overall, the emergence of medical deserts is jointly affected by population distribution, road-network performance, and facility distribution.

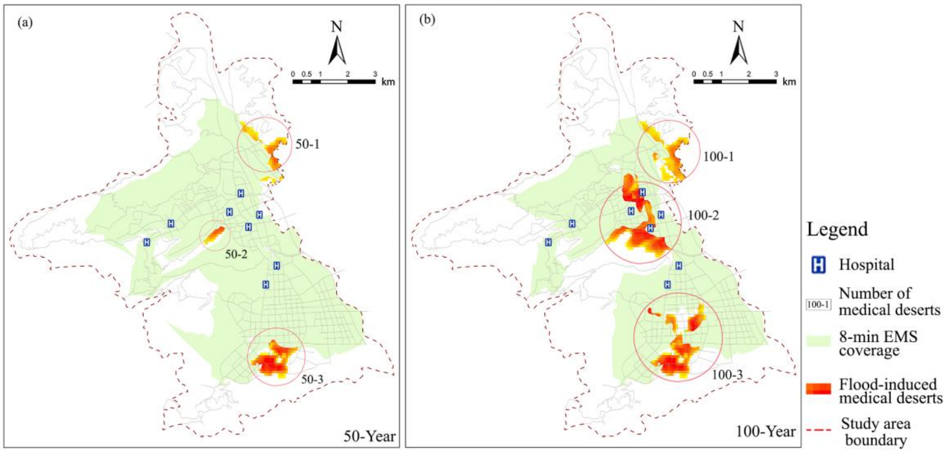

Figure 8: Identification of flood-induced medical deserts under (a) 50-year and (b) 100-year return-period events.

5 Discussion and planning implications

5.1 Discussion

(1) Nonlinear pluvial flood risk growth and the critical threshold.

The simulation results reveal a nonlinear relationship between flood intensity and risk in Mentougou New Town, with the 50-year event serving as a critical threshold. Below this threshold, inundation expansion is gradual and spatially contained. Beyond it, both inundation extent and the proportion of deep-inundation zones increase sharply. This pattern aligns with observations in other piedmont cities (Zhang et al., 2025), where topographic amplification and limited drainage capacity create abrupt shifts (Liu et al., 2018). Infrastructure designed only for lower return periods may therefore underestimate extreme risks in cities with complex terrain.

(2) Two-phase failure of road-network performance.

Road-network performance follows a two-phase attenuation pattern: speed reduction under 10-year and 20-year events, followed by structural connectivity loss under the 50-year and 100-year events. While many studies have modelled disaster-induced increases in travel time (He et al., 2026a), this study quantifies the mechanism of limited number of critical roads which represents only 3.2% of total network length can trigger a sharp decline in network efficiency.. This pattern is consistent with the vulnerability of road networks to targeted disruption (Dong et al., 2022). A critical finding is that moderately submerged secondary roads (0.3-0.5 m) do not cause equivalent system-wide effects. Resilience measures should therefore prioritise the protection of crucial roads rather than distribute investments to all roads.

(3) Spatial mismatch as the mechanism of medical deserts**.**

Medical deserts under pluvial floods arise not merely from road failures or high population density alone, but from their spatial mismatch. In Mentougou New Town, medical resources are concentrated in the central area. This centralised layout may offer economies of scale, but once flooding causes road disruptions, the peripheries lose both direct and alternative access. This finding extends the concept of double jeopardy observed in environmental justice literature (Rozhkov et al., 2025). Communities that are already disadvantaged in terms of resource distribution suffer severe consequences when an external shock damages the connection (Gotham, 2010).The spatial coincidence between the three

https://doi.org/10.5194/egusphere-2026-4082
Preprint. Discussion started: 21 July 2026

identified medical deserts (100-1, 100-2, 100-3) and the locations of interrupted crucial roads provides direct evidence that infrastructure-resource mismatches can become the dominant failure mechanism in extreme events.

(4) Unexpected resilience under low-intensity events and policy implications**.**

The finding shows that under 10-year and 20-year events, the 8-min service zone remains nearly intact (>98% of high-density areas covered), despite reductions in travel speeds. This suggests that the road network provides a buffer against moderate flood impacts. However, this buffer weakens under the 50-year event. From a policy perspective, the results challenge the common practice of using a single design return period for all infrastructure types The tiered resilience standard should be recommended: roads and emergency facilities in high-density peripheral zones should be designed to withstand at least the 50-year flood, while central facilities may maintain lower standards provided that redundant routes are guaranteed. The "dual-use for normal and emergency" transformation of existing community health centers in medical desert zones (e.g., in 100-1 and 100-2 area) would be a cost-effective first step.

5.2 Planning implications

The results suggest that improving EMS resilience under pluvial flood requires more than protecting individual hospitals. Based on the identified accessibility loss and flood-induced medical deserts, the following planning and management implications can be drawn.

(1) Improve the redundancy of emergency medical service provision.

Flood-induced medical deserts emerge where high population exposure overlaps with reduced road accessibility and limited medical alternatives. EMS planning should therefore avoid relying only on a small number of central hospitals. A more resilient strategy is to develop a hierarchical and flexible service network that can maintain basic emergency care when access to major hospitals is delayed. Disaster-oriented EMS planning should consider multi-coverage, service redundancy, and facility availability under disrupted conditions, rather than only normal-condition demand coverage (Yang et al., 2020) . Community health centres, township clinics, and temporary emergency stations can serve as supplementary medical nodes during extreme rainfall events. These facilities do not need to replace general hospitals, but they can provide triage, first aid, basic treatment, and patient transfer support. This is particularly important because adverse weather can reduce EMS accessibility and create areas with limited timely access to emergency care (Zhang et al., 2024). For areas repeatedly identified as potential medical deserts, emergency medical functions should be incorporated into routine facility planning and disaster preparedness.

(2) Protect critical access corridors rather than all roads equally.

The results indicate that EMS accessibility can be strongly affected by a limited number of roads. Flood mitigation for EMS should therefore shift from uniform road improvement to critical-corridor protection. Road criticality should be assessed not only by traffic volume or road hierarchy, but also by its role in maintaining access to critical facilities such as hospitals, ambulance stations, and emergency shelters (Gangwal et al., 2023b). In this study, roads that connect high-density communities with hospitals or alternative medical nodes should be prioritized for drainage improvement, maintenance, and emergency traffic management. Local measures, such as inlet improvement, temporary drainage support, and treatment of waterlogging-prone points, are especially important for low-lying corridors and narrow streets. At the network level, redundant routes and emergency detour plans should be prepared in advance. This is necessary because flood impacts on linear infrastructure can propagate beyond the directly inundated area through network interdependence and service disruption (Arrighi et al., 2021). The aim is not to eliminate all road inundation, but to prevent the failure of a few key links from isolating entire communities.

(3) Link flood early warning with EMS dispatch and resource pre-positioning.

The nonlinear decline in EMS accessibility suggests that emergency response should be adjusted before road disruption reaches a critical level. When rainfall forecasts indicate a high probability of severe road inundation, ambulances, medical

https://doi.org/10.5194/egusphere-2026-4082
Preprint. Discussion started: 21 July 2026

staff, and temporary response resources should be pre-positioned near areas with high population exposure and limited alternative access. Disaster risk management should evaluate infrastructure not only by its physical exposure, but also by its role in maintaining access to public services (Tariverdi et al., 2023). For EMS, dynamic dispatch should therefore incorporate real-time information on rainfall, inundation depth, road passability, hospital availability, and demand hotspots. Coordination between health, transport, water management, and emergency management departments is also needed. Rather than treating flood control, traffic management, and medical response as separate tasks, cities should develop joint contingency plans that define thresholds for resource deployment, route adjustment, hospital diversion, and inter-facility transfer.

Overall, the results highlight a general planning principle for flood-prone cities. EMS resilience depends on the joint configuration of medical facilities, road networks, population distribution, and emergency management capacity. For piedmont and other flood-prone urban areas with centralized medical resources and uneven road connectivity, risk-informed planning should identify potential medical deserts in advance, protect the corridors that maintain access to emergency care, and build flexible medical service capacity in vulnerable communities.

6 Conclusions

This study developed an integrated framework to assess emergency medical services (EMS) accessibility loss under pluvial flood by linking inundation simulation, road-network degradation, 8-min EMS coverage areas, and population exposure. Using Mentougou New Town as an empirical case, the analysis shows increasing rainfall severity can transform road-level disruption into population-level emergency care deficits. The main conclusions are as follows:

(1) The simulation of disaster-induced road disruptions indicates that a 50-year return period rainfall event is the critical point of the EMS. This implies the emergency system transitions from acceptable degradation to a functional collapse. And the Emergency medical transport is severely compromised.

(2) The spatial overlay of service boundaries and population data reveals the emergence of flood-induced medical deserts under extreme inundation events. High-density populations located away from the central medical core face a dual disadvantage: concentrated potential demand and weakened timely access to emergency medical care. This indicates that the presence of medical facilities does not necessarily ensure effective emergency access during flood events.

(3) The identification of failed road segments highlights that the inundation depth of critical road segments determines the survivability of the entire rescue network. Redundant road networks provide critical service and evacuation routes, ensuring that EMS remain accessible during extreme events.

(4) The assessment demonstrates that the degree of resilience of a city depends on a coordinated and balanced relationship between the elements that form a part of the process of urbanization. This indicates that mitigating spatial mismatch requires cities to adjust their strategic plans from conventional resistance to systemic resilience, ensuring the deep integration of spatial layout optimization, engineering enhancements, and emergency management synergy.

Future research should further refine the analysis of the impacts of population mobility and hospital capacity on emergency medical services under different disaster scenarios. In the context of increasingly frequent extreme climate events, urban emergency management systems are shifting from passive response to proactive and resilience-oriented adaptation (Wang et al., 2026). The methodological framework and empirical findings of this study offer a useful reference for other high risk-cities in conducting disaster risk assessments, optimizing emergency resource allocation, and supporting the development of climate resilient urban systems.

Data availability

All raw data can be provided by the corresponding author upon request (Xiaodong Guo :guoxd7797@163.com).

https://doi.org/10.5194/egusphere-2026-4082
Preprint. Discussion started: 21 July 2026

Author contributions

YY and XG planned the research. YY developed the methodology, conducted the flood simulation and accessibility analysis, and wrote the manuscript draft. LH contributed to data collection and preprocessing. CX and ZW contributed to spatial data processing, result visualization, and interpretation. XG, LH, CX, and ZW reviewed and edited the manuscript. All authors discussed the results and approved the final version of the manuscript.

Competing interests

The contact author has declared that none of the authors has any competing interests.

Disclaimer

Publisher's note: Copernicus Publications remains neutral with regard to jurisdictional claims made in the text, published maps, institutional affiliations, or any other geographical representation in this paper. While Copernicus Publications makes every effort to include appropriate place names, the final responsibility lies with the authors. Views expressed in the text are those of the authors and do not necessarily reflect the views of the publisher.

Acknowledgements

The authors would like to express sincere gratitude for the financial support from the Ministry of Education of Humanities and Social Science Project (Grant No. 25YJCZH297), the Beijing Municipal Natural Science Foundation (Grant No. 8232004), the Scientific Research Fund of the Institute of Engineering Mechanics, China Earthquake Administration (Grant No. 2026D23), and the Provincial University Basic Research Fund Project (Grant No. 2026JK018). The authors are also deeply grateful to the Mentougou District Government for their valuable assistance in field surveys and for providing data and materials. The field investigations were carried out in the Mentougou area, and the research benefited from the local research infrastructure and logistical support facilitated by the district government.

Financial support

The authors would like to express sincere gratitude for the support by the Ministry of Education of Humanities and Social Science Project (Grant No. 25YJCZH297); the Beijing Municipal Natural Science Foundation (Grant No. 8232004); the Scientific Research Fund of the Institute of Engineering Mechanics, China Earthquake Administration (Grant No. 2026D23); Provincial University Basic Research Fund Project (Grant No. 2026JK0 This research has been supported by the Deutsche Forschungsgemeinschaft (grant No. 390683824).

References

Abebe, Y. A., Pregnolato, M., and Jonkman, S. N.: Flood impacts on healthcare facilities and disaster preparedness – a systematic review, Int. J. Disaster Risk Reduct., 119, 105340, https://doi.org/10.1016/j.ijdrr.2025.105340, 2025.

Al-Qadami, E., Razi, M. A. M., Shah, S. M. H., Pu, J. H., Amran, M., Díaz Huenchuan, M. A., and Avudaiappan, S.: Floodwaters and vehicle hydrodynamics: a deep dive into risk mitigation unraveling vehicle stability in floods, Results Eng., 23, 102540, https://doi.org/10.1016/j.rineng.2024.102540, 2024.

Arrighi, C., Pregnolato, M., and Castelli, F.: Indirect flood impacts and cascade risk across interdependent linear infrastructures, Nat. Hazards Earth Syst. Sci., 21, 1955–1969, https://doi.org/10.5194/nhess-21-1955-2021, 2021.

Behrman, P., Fitzgibbon, M. L., Dulin, A., Wang, M. L., and Baskin, M.: Society of behavioral medicine statement on COVID-19 and rural health, Transl. Behav. Med., 11, 625–630, https://doi.org/10.1093/tbm/ibaa114, 2021.

Brînzac, M. G., Kuhlmann, E., Dussault, G., Ungureanu, M. I., Chereches, R. M., and Baba, C. O.: Defining medical deserts – an international consensus-building exercise, Eur. J. Public Health, 34, ckae144.1585, https://doi.org/10.1093/eurpub/ckae144.1585, 2024.

Chang, H., Lafrenz, M., Jung, I.-W., Figliozzi, M., Platman, D., and Pederson, C.: Potential impacts of climate change on flood-induced travel disruptions: a case study of portland, oregon, USA, Ann. Assoc. Am. Geogr., 100, 938–952, https://doi.org/10.1080/00045608.2010.497110, 2010.

Chen, R.-S. and Yang, K.-H.: Terraced paddy field rainfall-runoff mechanism and simulation using a revised tank model, Paddy Water Environ., 9, 237–247, https://doi.org/10.1007/s10333-010-0225-3, 2011.

Chen, Z., Zheng, C., Xu, M., Wu, Z., Zheng, S., and Ma, G.: Quantitative assessment of congestion diffusion and cascading effect under rainfall-flood disasters: a case study of Nanjing, china, Int. J. Disaster Risk Reduct., 114, 104915, https://doi.org/10.1016/j.ijdrr.2024.104915, 2024.

Dong, S., Gao, X., Mostafavi, A., and Gao, J.: Modest flooding can trigger catastrophic road network collapse due to compound failure, Commun. Earth Environ., 3, 38–47, https://doi.org/10.1038/s43247-022-00366-0, 2022.

Emami, S. G., Lorenzoni, V., and Turchetti, G.: Towards resilient healthcare systems: a framework for crisis management, Int. J. Environ. Res. Public. Health, 21, 286, https://doi.org/10.3390/ijerph21030286, 2024.

Ermagun, A., Smith, V., and Janatabadi, F.: High urban flood risk and no shelter access disproportionally impacts vulnerable communities in the USA, Commun. Earth Environ., 5, 2–9, https://doi.org/10.1038/s43247-023-01165-x, 2024.

Fang, B. and Gu, J.: Roads in rainstorms: a systematic optimization framework for overloaded road drainage sections, Water Resour. Manag., 40, 235, https://doi.org/10.1007/s11269-026-04626-y, 2026.

Gangwal, U., Siders, A. R., Horney, J., Michael, H. A., and Dong, S.: Critical facility accessibility and road criticality assessment considering flood-induced partial failure, Sustain. Resilient Infrastruct., 8, 337–355, https://doi.org/10.1080/23789689.2022.2149184, 2023a.

Gangwal, U., Siders, A. R., Horney, J., Michael, H. A., and Dong, S.: Critical facility accessibility and road criticality assessment considering flood-induced partial failure, Sustain. Resilient Infrastruct., 8, 337–355, https://doi.org/10.1080/23789689.2022.2149184, 2023b.

Golazad, S., Heravi, G., AminShokravi, A., and Mohammadi, A.: Integrating GIS, agent-based, and discrete event simulation to evaluate patient distribution policies for enhancing urban healthcare access network resilience, Sustain. Cities Soc., 111, 105559, https://doi.org/10.1016/j.scs.2024.105559, 2024.

Gotham, K. F.: Race, place, and environmental justice after hurricane katrina: struggles to reclaim, rebuild, and revitalize new orleans and the gulf coast, Contemp. Sociol. J. Rev., 39, 25–26, https://doi.org/10.1177/0094306109356659g, 2010.

Gou, L., Liu, Y., Zhang, Y., Zhu, Z., Peng, D., and Dou, J.: Estimating the instability criterion of vehicles in urban flooding by an entropic method, Urban Clim., 41, 101069, https://doi.org/10.1016/j.uclim.2021.101069, 2022.

Green, D., Yu, D., Pattison, I., Wilby, R., Bosher, L., Patel, R., Thompson, P., Trowell, K., Draycon, J., Halse, M., Yang, L., and Ryley, T.: City-scale accessibility of emergency responders operating during flood events, Nat. Hazards Earth Syst. Sci., 17, 1–16, https://doi.org/10.5194/nhess-17-1-2017, 2017.

Haghighatafshar, S., Becker, P., Moddemeyer, S., Persson, A., Sörensen, J., Aspegren, H., and Jönsson, K.: Paradigm shift in engineering of pluvial floods: from historical recurrence intervals to risk-based design for an uncertain future, Sustain. Cities Soc., 61, 102317, https://doi.org/10.1016/j.scs.2020.102317, 2020.

He, J., Guo, X., Wang, W., Xia, C., and Tong, A.: Modeling service flows in earthquake scenarios using a physical–social multilayer network, Reliab. Eng. Syst. Saf., 112800, https://doi.org/10.1016/j.ress.2026.112800, 2026a.

He, K., Carhart, N., Pregnolato, M., and De Risi, R.: Flood-induced traffic congestion and accessibility loss for urban road networks using agent-based simulation: the case study of bristol, UK, Int. J. Disaster Risk Reduct., 136, 106053, https://doi.org/10.1016/j.ijdrr.2026.106053, 2026b.

Hudson, P., Pham, M., and Bubeck, P.: An evaluation and monetary assessment of the impact of flooding on subjective well-being across genders in vietnam, Clim. Dev., 11, 623–637, https://doi.org/10.1080/17565529.2019.1579698, 2019.

IPCC (Intergovernmental Panel On Climate Change): Climate Change 2014: Impacts, Adaptation, and Vulnerability. Part A: Global and Sectoral Aspects. Contribution of Working Group II to the Fifth Assessment Report of the Intergovernmental Panel on Climate Change, edited by: Field, C. B., Barros, V. R., Dokken, D. J., Mach, K. J., Mastrandrea, M. D., Bilir, T. E., Chatterjee, M., Ebi, K. L., Estrada, Y. O., Genova, R. C., Girma, B., Kissel, E. S., Levy, A. N., MacCracken, S., Mastrandrea, P. R., and White, L. L., Cambridge University Press, Cambridge, United Kingdom and New York, NY, USA, 1132 pp., ISBN 978-1-107-64165-5, 2014.

Karamouz, M., Taheri, M., Khalili, P., and Chen, X.: Building infrastructure resilience in coastal flood risk management, J. Water Resour. Plan. Manag., 145, 04019004, https://doi.org/10.1061/(ASCE)WR.1943-5452.0001043, 2019.

Liu, Y., Yang, Z., Huang, Y., and Liu, C.: Spatiotemporal evolution and driving factors of China's flash flood disasters since 1949, Sci. China Earth Sci., 61, 1804–1817, https://doi.org/10.1007/s11430-017-9238-7, 2018.

Liu, Z., Li, S., Zhao, X., Wang, Z., and Chen, Y.: Examining accessibility to medical resources for urban older adults with common diseases using multisource data: a case study of Beijing, J. Urban Plann. Dev., 149, 5023031, https://doi.org/10.1061/JUPDDM.UPENG-4347, 2023.

Madakumbura, G. D., Thackeray, C. W., Norris, J., Goldenson, N., and Hall, A.: Anthropogenic influence on extreme precipitation over global land areas seen in multiple observational datasets, Nat. Commun., 12, 3944, https://doi.org/10.1038/s41467-021-24262-x, 2021.

Papilloud, T., Steiner, A., Zischg, A., and Keiler, M.: Road network disruptions during extreme flooding events and their impact on the access to emergency medical services: a spatiotemporal vulnerability analysis, Sci. Total Environ., 956, 177140, https://doi.org/10.1016/j.scitotenv.2024.177140, 2024.

Pareta, K. and Pareta, U.: A review of cloudbursts events in the himalaya region, and 2D hydrodynamic simulation using MIKE models, Nat. Hazards, 121, 9161–9193, https://doi.org/10.1007/s11069-025-07173-8, 2025.

Patro, S., Chatterjee, C., Mohanty, S., Singh, R., and Raghuwanshi, N. S.: Flood inundation modeling using MIKE FLOOD and remote sensing data, J. Indian Soc. Remote Sens., 37, 107–118, https://doi.org/10.1007/s12524-009-0002-1, 2009.

Pregnolato, M., Ford, A., Wilkinson, S. M., and Dawson, R. J.: The impact of flooding on road transport: a depth-disruption function, Transp. Res. Part Transp. Environ., 55, 67–81, https://doi.org/10.1016/j.trd.2017.06.020, 2017.

Rozhkov, A., Zandiatashbar, A., and Seyrfar, A.: Tackling transportation inequality through unveiling chicago's transit deserts and vulnerable communities, J. Urban Plan. Dev., 151, 4025030, https://doi.org/10.1061/JUPDDM.UPENG-5499, 2025.

Rufat, S., Tate, E., Burton, C. G., and Maroof, A. S.: Social vulnerability to floods: review of case studies and implications for measurement, Int. J. Disaster Risk Reduct., 14, 471–486, https://doi.org/10.1016/j.ijdrr.2015.09.013, 2015.

Tariverdi, M., Nunez-del-Prado, M., Leonova, N., and Rentschler, J.: Measuring accessibility to public services and infrastructure criticality for disasters risk management, Sci. Rep., 13, 1569, https://doi.org/10.1038/s41598-023-28460-z, 2023.

Tate, E., Rahman, M. A., Emrich, C. T., and Sampson, C. C.: Flood exposure and social vulnerability in the United States, Nat. Hazards, 106, 435–457, https://doi.org/10.1007/s11069-020-04470-2, 2021.

Vogelbacher, A., Von Szombathely, M., Lennartz, M., Poschlod, B., and Sillmann, J.: A high-resolution framework for urban pluvial flood risk mapping, Nat. Hazards Earth Syst. Sci., 26, 2765–2783, https://doi.org/10.5194/nhess-26-2765-2026, 2026.

https://doi.org/10.5194/egusphere-2026-4082
Preprint. Discussion started: 21 July 2026

Wang, Y., Hou, J., Li, D., Li, G., Pan, X., Lv, J., Fan, C., Sun, J., Yi, W., and Yang, Y.: Numerical simulation-based study on the response of urban drainage networks to flooding and road risk in typical plain city, J. Environ. Manage., 404, 129199, https://doi.org/10.1016/j.jenvman.2026.129199, 2026.

Xie, Z., Fu, X., Jiang, F., Deng, Z., Yin, S., Xie, X., Zhao, L., Wang, Q., Ji, C., Zheng, D., Lian, J., and Yuan, X.: Resilience levels of natural–social security in urbanization: a case study of Kunming, china, J. Urban Plan. Dev., 150, 5024029, https://doi.org/10.1061/JUPDDM.UPENG-4539, 2024.

Yang, Y., Yin, J., Ye, M., She, D., and Yu, J.: Multi-coverage optimal location model for emergency medical service (EMS) facilities under various disaster scenarios: a case study of urban fluvial floods in the minhang district of Shanghai, china, Nat. Hazards Earth Syst. Sci., 20, 181–195, https://doi.org/10.5194/nhess-20-181-2020, 2020.

Yin, J., Xu, S., Jing, Y., YIN'e, Z., and Liao, B.: Evaluating the impact of fluvial flooding on emergency responses accessibility for a mega-city's public services: a case study of emergency medical service, Acta Geogr. Sin., 73, 1737–1747, https://doi.org/10.11821/dlxb201809010, 2018.

Zhang, W., Wang, Y., Hu, Q., Sun, W., and Jin, J.: Comprehensive analysis on causes of flood disaster in megacities: a case study of Chongqing, J. Civ. Environ. Eng., 47, 1–10, https://doi.org/10.11835/j.issn.2096-6717.2023.090, 2025.

Zhang, Y., Liu, K., Ni, X., Wang, M., Zheng, J., Liu, M., and Yu, D.: Spatial accessibility of emergency medical services under inclement weather: a case study in Beijing, china, Nat. Hazards Earth Syst. Sci., 24, 63–77, https://doi.org/10.5194/nhess-24-63-2024, 2024.

Zhu, W., Zha, X., Luo, P., Wang, S., Xv, C., and Ji, Y.: Risk assessment of human and vehicle stability in extreme weather events in coastal cities, Water Resour. Manag., 39, 6351–6375, https://doi.org/10.1007/s11269-025-04253-z, 2025.